

Article

## Highly Sensitive and Miniaturized Fluorescence Detection System with an Autonomous Capillary Fluid Manipulation Chip

Mingjin Yao <sup>1,\*</sup>, Girish Shah <sup>2</sup> and Ji Fang <sup>1</sup>

<sup>1</sup> Institute for Micromanufacturing, Louisiana Tech University, Ruston, LA 71270, USA;  
E-Mail: jfang@latech.edu

<sup>2</sup> College of Pharmacy, University of Louisiana at Monroe, Monroe, LA 71209, USA;  
E-Mail: shah@ulm.edu

\* Author to whom correspondence should be addressed; E-Mail: mya003@latech.edu.

Received: 10 April 2012; in revised form: 27 April 2012 / Accepted: 9 May 2012 /

Published: 10 May 2012

---

**Abstract:** This paper presents a novel, highly sensitive and ultra-small fluorescent detection system, including an autonomous capillary fluid manipulation chip. The optical detector integrates a LED light source, all necessary optical components, and a photodiode with preamplifier into one package of about 2 cm × 2 cm × 2 cm. Also, the low-cost and simple pumpless microfluidic device works well in sample preparation and manipulation. This chip consists of capillary stop valves and trigger valves which are fabricated by lithography and then bonded with a polydimethylsiloxane-ethylene oxide polymer polydimethylsiloxane (PEO-PDMS) cover. The contact angle of the PEO-PDMS can be adjusted by changing the concentration of the PEO. Hence, the fluidic chip can achieve functionalities such as timing features and basic logical functions. The prototype has been tested by fluorescence dye 5-Carboxyfluorescein (5-FAM) dissolved into the solvent DMSO (Dimethyl Sulfoxide). The results prove a remarkable sensitivity at a pico-scale molar, around 1.08 pM. The low-cost and miniaturized optical detection system, with a self-control capillary-driven microfluidic chip developed in this work, can be used as the crucial parts in portable biochemical detection applications and point of care testing.

**Keywords:** highly sensitive; fluorescence detection; miniaturization; microfluidics; capillary stop valve; lab-on-a-chip; hydrophilic PDMS

---

## 1. Introduction

In the 1990s, microfluidic technologies and lab-on-a-chip were perceived as having potential to be powerful applications due to their advantages of their small size, low volume requirement for samples, and accurate analysis. Furthermore, integrating fluid actuation, sample pre-treatment, sample separation, signal detection, and signal amplification into a single device have been highly developed [1]. Based on these technologies, currently many bio-detection systems are widely studied, such as the electrochemical method, refractive metrology, fluorescent detection, conductive detection, infrared detection, Raman detection, and mass spectrometry, which have been presented in other researchers' papers, e.g., [2]. However, fluorescence-based detection is the most used because of its inherently high sensitivity, selectivity and efficiency for detection. The fluorescence detection uses a certain wavelength and high energy beam such as a laser or LED to excite unknown sample characters with a fluorescent label [3,4]. By reading the emitted fluorescent intensity from labels, the unknown concentration of sample target per unit volume can be obtained [5,6]. In order to achieve the high sensitivity, conventional bio-fluorescent systems usually adapt a charge-coupled device (CCD) camera, detection microscopy [7] and photomultiplier tubes, which are expensive and do not match the size of microchip and portable systems [8] even though they are sensitive. If the diagnostic tools could be miniaturized, made easy to use, less expensive, and also readily available at the point of need such as emergency diagnosis, millions of people would benefit from them. There are some publications available concerning the miniaturized detection system. One of the presented methods used for the portable detection systems integrates optical fiber on a chip to form an excitation light platform for fluorescent light detection with disposable microfluidic chips [5]. Another paper presents a system which integrates a sensor fabricated using CMOS technology with SU8 lens and a V-shaped inclined mirror and performed successfully to build a micro-fluorescence detection chip [9]. These systems have a low sensitivity, because they are difficult to fabricate and integrate all optics on a chip by MEMS technology. Thus, the existing systems are either too large or have a low sensitivity. Controlling the signal to noise ratio is especially hard, and they do not filter the unwanted light so that they are not favorable to the high sensitivity portable detection system. Only a few research papers have reported a miniaturized detection system, assembled and integrating optical components found in the commercial market [10,11]. The size of the system is about 5 cm × 5 cm × 5 cm with two 3 cm long tubes, and the sensitivity is about 1.96 nM. As they stand, there is a need to design a miniaturized detection system for the corresponding applications. The miniaturization of medical technologies has the potential to improve public health detection, and perhaps even to change the basic methods by which patients are diagnosed and treated [12]. This kind of detection system must be an inexpensive, portable and, ideally, uses compact instrumentation that consumes less power.

During the last two decades microfluidic systems have attracted much interest in various fields, such as chemistry, biology, and medicine [13]. In recent years, they have been widely used in the lab-on-a-chip and micro total analysis system ( $\mu$ TAS) for bio/chemical analysis applications on biotechnology, drug discovery, and environmental monitoring [14–18]. However, the integration and miniaturization of systems are the major challenges for researchers. The concept here is to use photolithography to fabricate the bio-laboratory into a silicon chip, which includes microreactors, mixers, micropumps, and microvalves. The photolithography for micromachining has been commonly

applied to miniaturize the chemical, biochemical, and biomedical analysis systems. This kind of microfabrication is a useful method to fabricate the miniaturized devices. Some reports have demonstrated the general advantages of miniaturized systems, compared to conventional large synthesis devices [19–23]. The miniaturization of these systems has many merits, such as the small volume reagents/sample consumption, reliability, automatic performance control, and portability at the point of care, which are beneficial to the bio/chemical analysis. Currently, the capillary action phenomenon is of great interest in the microfluidic research area because of its simple fluid flow control without extra pumps. Therefore, fluid control devices such as stop valves have become a main focal research topic in the capillary fluidic system. Many valve schemes have already been presented [24]. They can be categorized into active and passive types. The active valve [25] usually contains the closure parts, such as membranes or pistons, and is actuated by pneumatic, thermal or electrokinetic methods. These methods either require an external actuation mechanism, such as piezoelectric, electrostatic, and electromagnetic, or are very sensitive to the physicochemical properties of the components and other factors. These factors usually result in high costs, complexity in integration, difficulty in implementation, and a complicated fabrication. The passive valve [26] works with the surface tension and the energy balance principle, which has some advantages, such as no external power supply, the possibility of use without an active control, easily integrated, continuity in substrate material, and a low cost. However, the passive valve still strongly depends on the variances in the fabrication process and is not suitable for all of the fluidic mediums. There are two main methods to make the capillary stop valve. One method is to make the channel surface hydrophilic and the substrate surface of the valve hydrophobic for the enhancement of the resistance to stop the liquid at the opening of the valve [27]. The other kind of capillary valve does not need an additional process to deposit a hydrophobic coating. It only relies on the surface tension and the static contact angle of the interface of the channel surface and the liquid viscosity [28]. Thus, the control of the burst pressure barrier is dominant over the other parameters in the fluid flow manipulation. A few publications have mentioned its successful utilization in chemical and biological analysis system units [29]. The predetermined volumes of liquid sample to a point of use are precisely delivered by the combination of the capillary filling with stop valves [30–34]. In addition, the cover sheet bonding to the microchip is also critical in the design. At present, the microchip with capillary channels and stop valves often utilizes glass as a cover. However, it is hard to drill the holes as the inlets and outlets into the glass cover of the device. Moreover, the ordinary glass is usually much more hydrophilic so that the liquid may not stop at the opening of the stop valve, but it is good for liquid flowing fast in the capillary channel. Another cover sheet for the microchip is the widely used ordinary PDMS, which is very hydrophobic (contact angle is over  $102^\circ$ ) which makes the liquid flow slowly and even stop moving forward in the capillary channel sometimes. According to these existing difficulties of designing the effective capillary channel and stop valve, we propose a hydrophilic surface modified PDMS, which is used as the microchip cover and adjusts the contact angle of the PDMS to balance the fluid flowing in capillary channels as well as to be stable and stationary at the valve opening. This method provides an easy way to design a simple capillary microfluidic system for different applications in biomedical and chemical analysis instruments.

This paper presents a low cost, high sensitivity and miniaturized fluorescence optical detection system with an autonomous fluid manipulation chip which solves the existing bottleneck of current

detection system as low sensitive or large-size for the biochemical applications of portable device/system, lab-on-a-chip and point care. This system includes two parts: optical assembly and detector with preamplifiers. Optical assembly conducts the excitation light path and emission or detection light path. Each path has a light filter for passing the light of excitation or emission wavelength only. The dichroic mirror and some lenses are necessary to complete the fluorescent detection. All components are assembled into a metal house about  $2\text{ cm} \times 2\text{ cm} \times 2\text{ cm}$ . For eliminating the noise, a photodiode with preamplifier and one more amplifier is assembled on a small print circuit board ( $2\text{ cm} \times 2\text{ cm}$ ). The transimpedance of the detector is about  $5\text{ G}\Omega$ . This prototype has been tested using fluoresce dye 5-Carboxyfluorescein (5-FAM), which is injected into an autonomous fluidic manipulation chip. The results show that the sensitivity of this system is around  $1.08\text{ pM}$ . This range of sensitivity should meet most of the bio-detection requirements. This system can also be applied in medical, protein detection, PCR, DNA extraction. However, the autonomous fluid manipulation chip in our study focuses on the design and fabrication of passive microfluidic stop valves. Meanwhile, the modified PDMS with a hydrophilic property, which is used as the cover sheet of the microfluid chip, is also investigated. The testing of the capillary stop valve sealed with the surface modified PDMS in the experiments will be described in later sections. The principle of the capillary-driven stop valves is understood by considering a surface energy balance which is compensated by a great deal of manipulation performed against the Laplace pressure. The type of capillary-driven stop valve described here is pumpless, without external actuators. It includes two main parts: a rectangular microchannel associated with a stop valve and the PEO-PDMS sheet bonded as a cover. The PEO-PDMS is easily used and readily adjusts the surface static contact angles with the surfactant inside. The PDMS surface treatment with PEO surfactant would change the contact angle of the regular PDMS to become hydrophilic and make the liquid flow in the microchannel. The liquid starts from the inlet, moving forward smoothly with a proper surface tension in the microchannel. At last, it stops at the opening of the microvalve. For the modification of the regular PDMS, the concentration of the surfactant additive is crucial. Different concentrations will have different effects, such as the different fluid flowing time in the capillary channel or the different fluid stationary time at the opening of the microvalve. All of the testing results are presented in detail in the following sections.

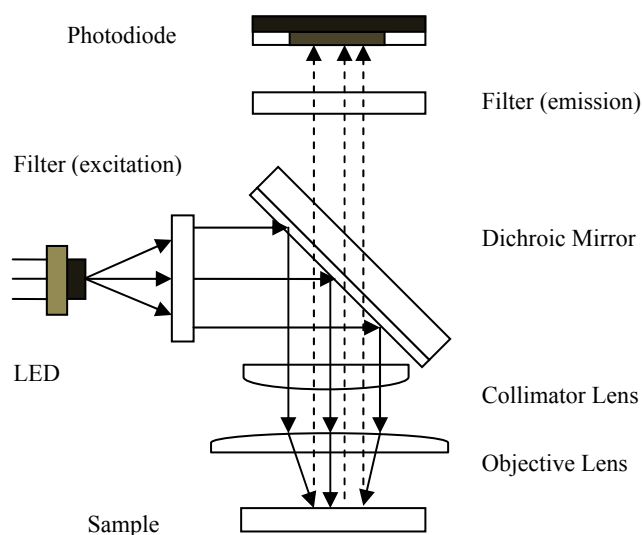
## 2. Design of the System

The proposed optical system for the fluorescence detection contains a light source which emits light at an appropriate wavelength ranging mainly around  $466\text{--}470\text{ nm}$ , an objective lens, a collimator lens, a dichroic mirror, an excitation filter, an emission filter and a photodetector built in the preamplifier in the optical path of the system. The excitation filter eliminates the unneeded light. The dichroic mirror is used for the light split of the excitation and the emission light path. The structure of the optical path in this system is shown in Figure 1.

The light emitting diode (LED) is applied as the light source in this system due to its advantages. In the past few years, the fluorescence detection system based on light emitting diodes (LED) became very popular because of its low cost [35]. LED is much cheaper than the other light sources, and it also has a long lifetime [8]. Here we reviewed various advantages of using LED lighting in detail. Early LEDs emitted a low-intensity red light, but modern versions are available across the visible, ultraviolet

and infrared wavelengths, with very high brightness. LED can be integrated into our portable detection optical system as it is only a few millimeters in diameter as well as in length so that it may be easily installed. It is also easily obtained in the commercial market, with a low replacement costs every 10 or more years, and up to 100,000 h life time which is approximately 14 years 18 h per day usage. Moreover, it uses 80% less energy consumption than most conventional lighting products and very durable with a very low maintenance record that is hard to break. So the small-sized LED products have become the common replacement for many types of conventional lighting applications. They are very economic and energy efficient with no wasted light or heat. There are many merits mentioned above, such as small size, long lifetime, fast switching, low energy consumption, robustness, and improved durability, reliability. They are also used in applications as diverse as replacements for aviation lighting, automotive lighting as well as in traffic signals. The compact size, the possibility of narrow bandwidth, switching speed, and extreme reliability of LEDs has allowed the new text and video displays and sensors to be developed, while their high switching rates are also useful in advanced communications technology. Infrared LEDs are also used in the remote control units of many commercial products including televisions, DVD players, and other appliances. They are mostly single-die LEDs used as indicators, and they come in various-sizes from 2 mm to 8 mm, through-hole and surface mount packages, which are usually simple in design, not requiring any separate cooling body. Typical current rating ranges from around 1 mA to above 20 mA. The small scale sets a natural upper boundary on power consumption due to heat caused by the high current density and the need for heat sinking [36].

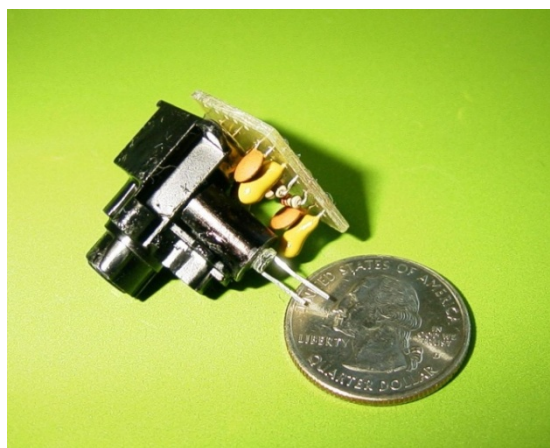
**Figure 1.** Structure of optical path in the system.



The prototype of the system is shown in Figure 2. The optical path of the system takes advantage of the dichroic mirror, excitation filter and different functional lenses to pass the light to the photodiode which collects the emitted signals from the samples. The optical path starts with a blue LED light source. This system employs a water clear colored LED model ETG-5MN470–15, which has a peak emission wavelength of 470 nm with a luminous intensity of 3 cd (candela), and a viewing angle of 15°. Then the light passes through the excitation filter and is reflected from the dichroic mirror,

which lets the light with 470 nm wavelength go through a collimator and an objective lens to focus on the sample. Then the fluorescence light about 518 nm wavelength from the sample is collimated by the same collimate lens, passes through the dichroic mirror, and is detected by a photodiode after being filtered by an emitter filter. The signal from the photodiode is immediately amplified by the amplification stage in the preamplifier, which is integrated in the photodiode-preamplifier.

**Figure 2.** The picture of the system.



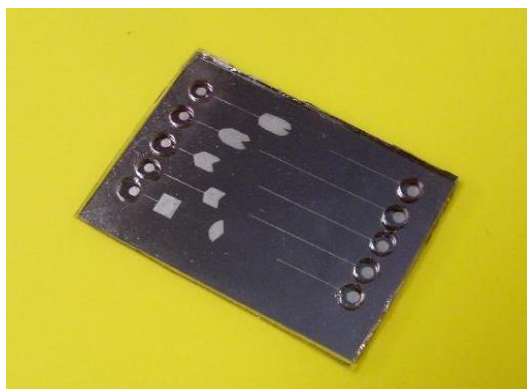
One of the most important components in an optical detection system is the photodetector. The major classes of photodetectors include photodiodes (PDs), charge-coupled devices (CCDs), photomultiplier tubes (PMTs), and avalanche photodiodes (APDs) [37,38]. Currently the photodiode (PD) and the photomultiplier tube (PMT) are the two common and versatile optical detectors. They have complementary capabilities and are very popular in optics. Both of them absorb light quanta (photons) and produce a current that is proportional to the rate of photon absorption. Also, there are some other common optical detection devices, including bolometers and pyroelectrics (both of which respond to the heat deposited by light absorbed in the detector), CCDs (charge-coupled detectors, used in digital cameras), photoconductors, vidicons (the original TV camera tubes), avalanche photodiodes, and phototransistors. They are all useful in the microfluidic detection area, which are also really very favorable on the familiar silicon photocell used in solar power conversion. Among all of these photodetectors, the photodiode is operated for optimum sensitivity and accuracy, suitable for the system we discussed. However, all these detectors are expensive and very large, and compatible with portable systems. Hence, in this project we have selected a blue/green enhanced 5 mm<sup>2</sup> silicon photodiode-preamplifier model ODA-6WB-500M, which features a large active area with extremely low noise, and high-sensitivity. The combination detector-preamplifier has a sensitivity of wavelength response at 450 nm, typically 315 V/ $\mu$ W. It operates between 400 nm and 1,100 nm with peak frequency response at 940 nm and features 500 Mohm transimpedance gain. It is easily integrated in an optical housing, and is ideal for fluorescence detection of low-light-level medical diagnostic applications because it has a few advantages over other systems. For example, the combined amplifier reduces both the outside and inside electrical and light signals interference, thus, it enhances the ratio of signal and noise, as well as increasing the sensitivity of this system. Another advantage is quite effective for the biomedical detection system. The emitter filter is mounted on it to filter the incident fluorescence light, then to generate the corresponding voltage to display on the multimeter which is

processed by the low-noise amplifier and analog-digital converter inside the photodiode. However, it usually should be operated in (complete) darkness.

The schematic illustration of the optical path in the system is shown in Figure 1. All the lenses and mirror devices are mounted mechanically to the housing and connected to each other to form a stable and miniaturized system. Figure 2 shows the picture of the system.

The design and fabrication of the microfluidic chip is presented in the following section. The microfluidic chip fabrication is performed in a clean room. The designed devices are fabricated on a single crystal silicon wafer (100 mm diameter, 500  $\mu\text{m}$  thick) with a 0.6  $\mu\text{m}$  thick silicon oxide layer. The channel and valve patterns on the wafer are fabricated by the standard photolithography process associated with the buffered oxide wet etching (BOE) and inductively coupled plasma (ICP) dry etching [39]. In the beginning, the wafer is placed on a hot plate for about half an hour at 250  $^{\circ}\text{C}$  for the hard bake. After the wafer is cooled, an approximate 2  $\mu\text{m}$  thick photoresist is spin-coated on it. The wafer is then soft baked at 90  $^{\circ}\text{C}$  for one minute. The mask aligner machine MA6 is used to transfer the pattern of the capillary channel and the stop valve from the mask to the photoresist by UV light. Then it is developed in a microposit MF-319 developer solution to define the distinct pattern. After that, it is cleaned with deionized (DI) water and blown dry to bake at 115  $^{\circ}\text{C}$  for one minute. These above steps are performed on the  $\text{SiO}_2$  layer. The photoresist layer is used as an etching mask, and the  $\text{SiO}_2$  layer is etched in a BOE solution. After the BOE, inductive coupled plasmas (ICP) dry etching is used to etch 230  $\mu\text{m}$  deep channels and valves in the silicon. Here, the standard Bosch process is applied [40,41], which makes high aspect ratio silicon structures with vertical sidewalls possible [42]. Finally, the low pressure  $\text{SF}_6$  plasma generated by a radio-frequency (RF) source is used to clean the  $\text{C}_4\text{F}_8$  deposition layer on the substrate and the walls of the channel and the valve. Due to these fabrication processes, the substrate and sidewalls of the pattern are smoother and more hydrophilic than the one without  $\text{SF}_6$  plasma cleaning.

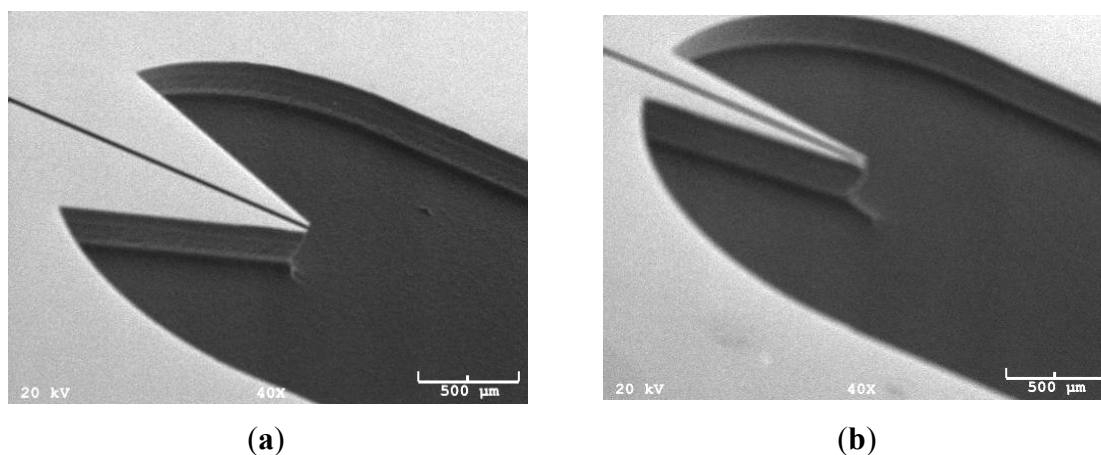
**Figure 3.** The capillary channels and microvalves patterns are fabricated on a chip.



The PDMS cover applied here is the surface modified hydrophilic PEO-PDMS, and the process of the PEO-PDMS preparation is presented in the next section “Experimental Results and Analysis”. Then, the silicon chip and PEO-PDMS are finally bonded together. Also, the surface of the PEO-PDMS is hydrophilic and favorable for the liquid flowing through the microchannels on the Si wafer [43]. Therefore, the PEO-PDMS is used to seal the fabricated device. The fabricated device is shown in Figure 3. Each chip has five capillary channels and six valves in different configurations.

Additionally, the profiles of the capillary channel and the stop valve are observed by scanning electron micrographs (SEM) in Figure 4. The etching depths are measured by a KLA tencor profilometer (TENCOR Alpha step 500 profiler; TENCOR Inc.) with a precision of  $\pm 0.01 \mu\text{m}$ .

**Figure 4.** SEM images of the etched capillary channel and stop valve profile. (a) The capillary channel is  $10 \mu\text{m}$  wide and the expanding angle of the stop valve is  $170^\circ$ . (b) The capillary channel is  $15 \mu\text{m}$  wide and the expanding angle of the stop valve is  $150^\circ$ .



### 3. Experimental Results and Analysis

We did a set of experiments using a dilution series of fluorescence dye in DI water conducted at room temperature in order to investigate the capability of the designed fluorescence [10] detection system. A kind of fluorescence dye called 5-Carboxyfluorescein (5-FAM), which is orange solid, was used in this testing experiment. 5-FAM is one of the most popular green fluorescent reagents used for biological and biomedical applications, such as *in situ* labeling peptides, proteins and nucleotides. It has also been used to prepare various small fluorescent molecules. It has the spectral properties whose absorbance wavelength is 492 nm, emission wavelength is 518 nm. The solvent liquid that can be used here is DMF or DMSO. DMSO (Dimethyl Sulfoxide) was applied in our experiment. It is a colorless liquid that dissolves both polar and nonpolar compounds and is miscible in a wide range of organic solvent as well as water.

The original sample solution was prepared by dissolving 0.5 mg 5-FAM into 1 mL dimethyl sulfoxide liquid and then stirring them uniformly with sonication. Then take  $70 \mu\text{L}$  of the original solution was diluted by adding DI water. Then each time portions of the previous sample were further diluted with DI water for the next testing. At last, the sample droplet was dripped onto the templet glass under the objective lens. The pipet was used to quantify the sample for the same dose every time. The dilution series started from a concentration of  $86.92 \mu\text{M}$  down to  $1.08 \text{ pM}$ . The amplitude of the fluorescence signal was reflected by the voltage difference measured since the signal collected by the photodiode was converted to the electrical signal be shown the output. The plot of the fluorescein solution's concentrations *versus* the voltage differences within a long range interval of the concentration ( $10 \times 10^{-8}$  to  $10 \times 10^{-12}$ ) is shown in Figure 5. We found the limit of detection of fluorescein to be  $1.08 \text{ pM}$ . In the meantime, the samples of the detailed different concentrations were also tested and then the curves were plotted in every different scale as shown in Figure 6 to Figure 10.

**Figure 5.** The relationship of the concentrations of the fluorescein solution samples range from  $10 \times 10^{-8}$  to  $10 \times 10^{-12}$  scale and the voltage differences.

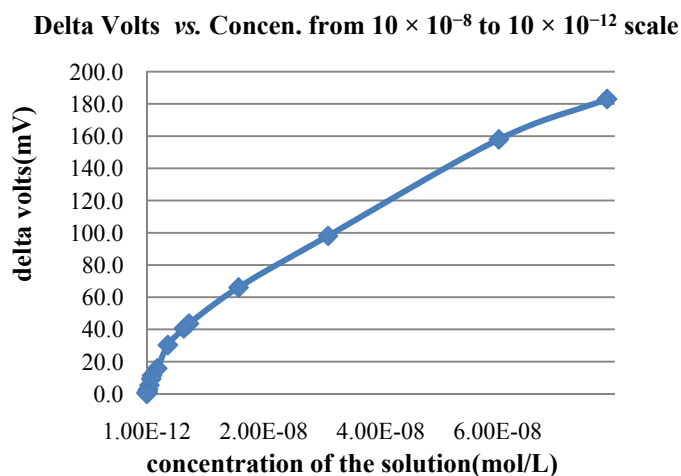


**Figure 6.** The relationship of the concentrations of the fluorescein solution samples and the voltage differences in  $10 \times 10^{-8}$  scale.

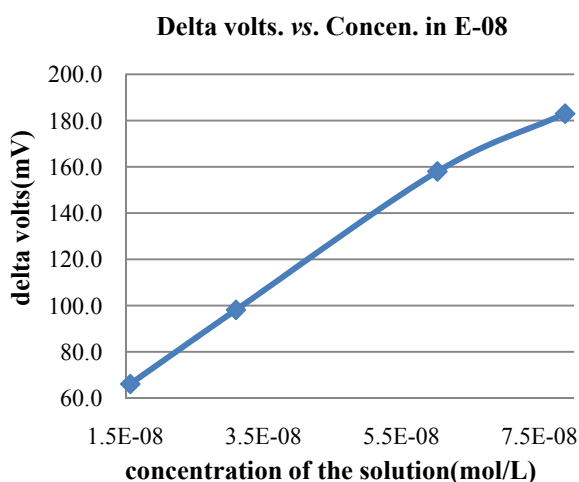


**Figure 7.** The relationship of the concentrations of the fluorescein solution samples and the voltage differences in nano-scale  $10 \times 10^{-9}$ .

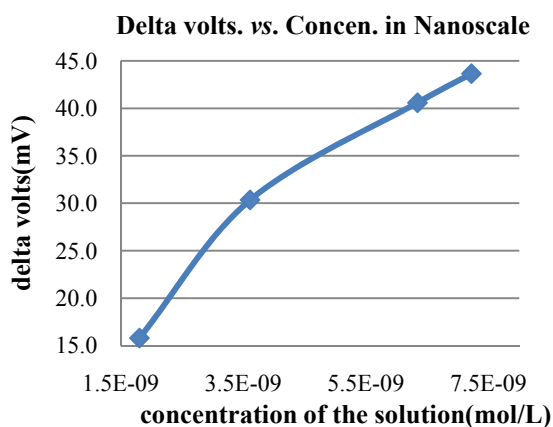


**Figure 8.** The relationship of the concentrations of the fluorescein solution samples and the voltage differences in  $10 \times 10^{-10}$  scale.

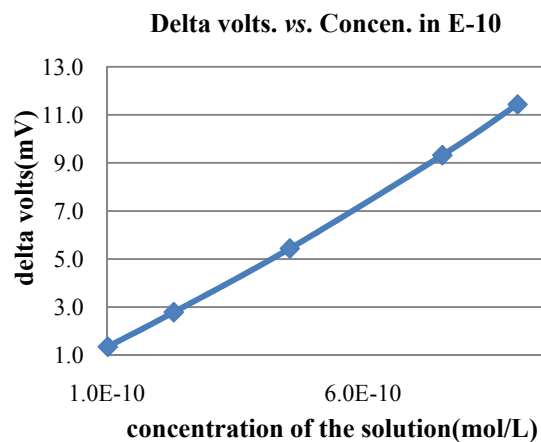


**Figure 9.** The relationship of the concentrations of the fluorescein solution samples and the voltage differences in  $10 \times 10^{-11}$  scale.

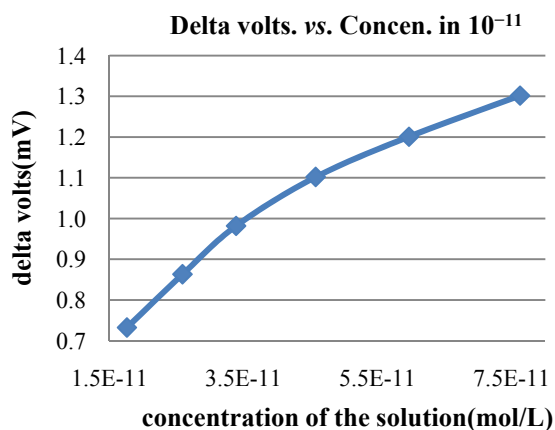
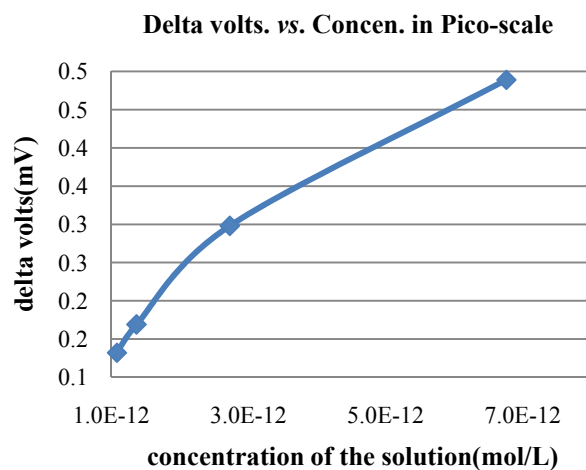


**Figure 10.** The relationship of the concentrations of the fluorescein solution samples and the voltage differences in pico-scale  $10 \times 10^{-12}$ .



From the plots we can see that the higher the concentration of the sample solution, the greater the voltage output will be, as we expected. When the concentration of the solution sample is increased, the corresponding voltage increases, too. A higher concentration of the sample solution causes a higher output voltage, determining the intensity of the signal we collect. As we have tested, the sensitivity of the system is impressive at almost 1.08 pM. On some certain level, this is enough for the actual bioassay testing and detecting application. The sensitivity could also be increased by improving the housing of the system or the influence of the ambient light area. However, the operation of detection should be cautious, such as the adjustment of the focus lens, and so on. These factors all impact the testing and detecting results.

**Figure 11.** Static water contact angles of the PEO-PDMS (PEO concentration is 0.2%–1.9% to the PDMS base polymer).

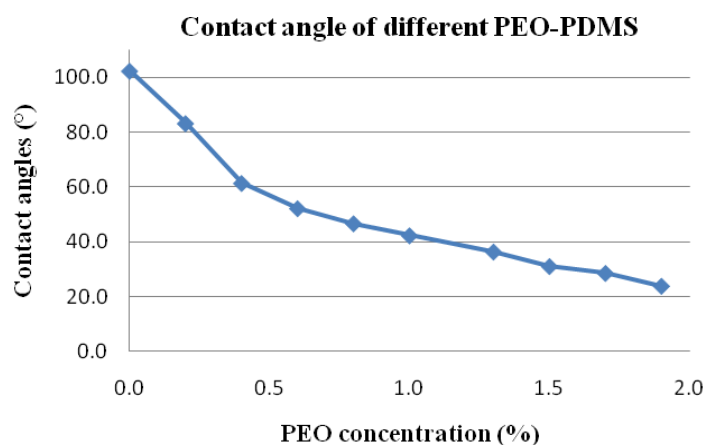
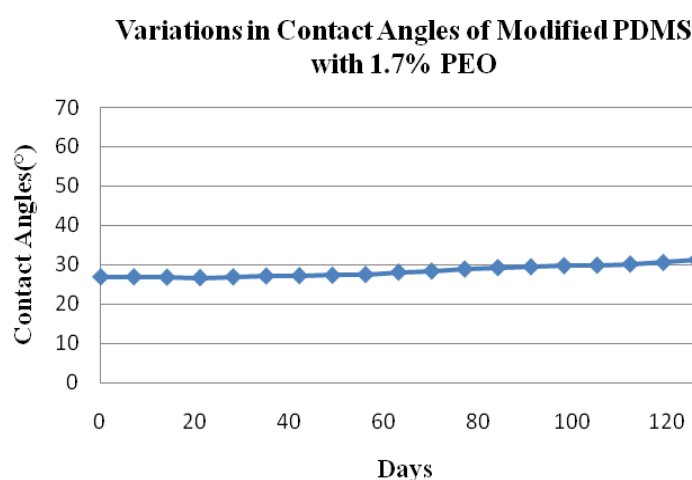


**Figure 12.** The curves are the days *versus* contact angles which illustrate the stability of the PEO-PDMS hydrophilicity.



The testing sample in the optical fluorescence detector is injected into the microfluidic chip which is fabricated by lithography. Also, the fabrication of the PEO-PDMS is one of the main parts, which changes the contact angle of the PDMS in order to control and balance the fluid flow in the microchannel and valve as the cover sheet of the autonomous microfluidic chip. In the previous experiments, we have tried the glass and the original PDMS bonded onto the fabricated silicon wafer,

respectively. But the glass is too hydrophilic to enable the valve to function well and the original PDMS is too hydrophobic to make the fluid flow stop moving in the capillary channel. Thus, the hydrophilic PDMS modification is proposed to control the contact angle of the interface and better control the surface tension inside the device. The hydrophilic PEO-PDMS monoliths can be successfully prepared by incorporating a small amount of PDMS-b-PEO block copolymer to a PDMS polymer base and the curing agent with a simple one step mixing method. This method was mentioned in the publication [44]. The PDMS-b-PEO is a surfactant additive in the PDMS hydrophilic surface treatment. The method of preparing the hydrophilic elastomers involves the synthesis of PDMS with tunable hydrophilic surface properties. The PDMS-b-PEO surfactant additive chain segment lengths are varied to control the hydrophobic/hydrophilic balance. Regular PDMS surfaces with tethered PEO block copolymers exhibit a dynamic surface where the wettability changes very rapidly. In this study, various PEO-PDMS mixtures are made with the different PDMS-b-PEO concentrations from 0.2% to 1.9% (the percentage to the PDMS base polymer in weight). The concentrations of 0.2%, 0.4%, 0.6%, 0.8%, 1.5%, 1.7%, and 1.9% are never tried in other publications. In order to investigate the hydrophilic property of the PEO-PDMS, the contact angles are measured. One droplet of the DI water with 1  $\mu\text{L}$  is dispensed on the PEO-PDMS surface, and the static contact angles are measured by an OCA40 contact angle meter and contour analysis system in Figure 11. Figure 12 shows the stability of the static water contact angle behavior on the modified PDMS surfaces with the PEO additive. The hydrophilic property of PEO-PDMS can usually last for a few months.

**Table 1.** The meniscus moving in the capillary channel (100  $\mu\text{m}$  wide, 28 mm long) with different velocities due to the different PEO-PDMS of different contact angles.

Concentrations of PDMS-b-PEO	Contact angles(degree)	Velocity( $\mu\text{m/s}$ )
0	106.5	0
0.2%	80.9	83.4
0.4%	58.5	540.9
0.6%	50.3	980.5
0.8%	43.8	4,800.8
1.0%	35.7	8,552.7
1.3%	32.9	9,002.3
1.5%	30.6	9,458.9
1.7%	26.8	9,971.5
1.9%	21.5	10,139.6

As for the investigation of the fluid flow and the measurement of the liquid flow velocity in the capillary channel, a capillary channel with 200  $\mu\text{m}$  in depth, 100  $\mu\text{m}$  in width, and 28 mm in length is fabricated on a silicon wafer and bonded with the PEO-PDMS (PEO concentration at 1.5%, 1.7%, 1.9%) cover. The best bonding for the PEO-PDMS (PEO concentration at 1.0%–1.9%) with a silicon wafer can be achieved after 15 s of the oxygen plasma treatment under the oxygen flow at 5 sccm, the RF power at 50 W, and the chamber pressure at 200 mTorr. For the enhancement of the bonding strength, the bonded PEO-PDMS and Si-wafer can be heated for 40 to 50 min at 90  $^{\circ}\text{C}$  on a hot plate. After that, this device can be ready for testing the fluid flow in channels. The velocities of the fluid meniscus in the channel are recorded by an i-SPEED 2 high speed video camera, which is an important

tool for general research and development requirements, with recording rates of up to 33,000 fps and instant playback analysis. Finally, the testing results are obtained and the meniscus velocities are listed in Table 1, which indicate that the higher the concentration of PEO in the PEO-PDMS cover sheet, the faster the fluid meniscus moves in the capillary channel. Also, it is indicated that when the PEO concentrations are more than 0.8%, the velocities increase dramatically in the capillary channels. Here, we take different concentrations for testing in comparison with the different velocities to verify that the contact angles will affect the fluid flowing in the capillary channels.

To test the stop valve, the capillary channel and stop valve are fabricated in a silicon wafer and have a size of 230  $\mu\text{m}$  in depth and 15  $\mu\text{m}$  in width. However, there are six different expanding angles of stop valves including 60°, 90°, 110°, 130°, 150°, 170° on a chip (Figure 3). Then, this chip is bonded with the PEO-PDMS, which has different concentrations of PEO. The red-colored DI water is used as the testing sample solution. After these preparations, the sample liquid is dropped into the inlet by a pipette and then auto-injected into the capillary channel. Finally, we observe the phenomenon of the fluid meniscus moving inside the capillary channel and valve. Table 2 lists the stationary time of the liquid meniscus at the opening of the stop valve corresponding to different stop valve sizes when the PEO concentration is 0.4%, which is the time of the meniscus pinned at the edge of the valve. The detailed explanation can be found in Gliere and Delattre's paper [45]. Table 3 states that the higher the concentration of the PEO, the shorter time the liquid stays at the opening of the stop valve. Table 4 shows that the different aspect ratios have influence on the meniscus stationary time at the opening of the capillary valve which agrees with the theory mentioned in Section 2. Tables 4 and 5 also give the velocities of the fluid meniscus in the capillary channels with different aspect ratios and bonded with the same PEO-PDMS, which will result in different velocities. From the data, it is obvious that the lower the aspect ratio, the faster the fluid meniscus moves in the microchannels. Because the contact angle of the PEO-PDMS with 0.4% PEO concentration is 58.5°, which is much lower than that of the silicon wafer (about 90°), the contact angle of the PEO-PDMS cover is dominant over the bottom substrate and the other two sidewalls of silicon in the microchannel. Thus, the aspect ratio will impact the fluid meniscus stationary time at the edge of the stop valve, which is listed in detail in Tables 4 and 5. We can see that the higher the aspect ratio, the longer time the fluid meniscus is pinned at the opening of the stop valve. Then the stop valve functions very well in this case of high aspect ratio. Figure 13 show the picture sequences taken with a high speed camera and illustrate the different positions of the liquid meniscus moving in the capillary channel and finally stop at the opening of the passive valve. From the data, we can find that the testing results coincide with the theoretical prediction: the bigger expansion angle of the stop valve, the longer the stationary time will be. The lower the contact angle of the PEO-PDMS, the faster the fluid meniscus moves in the capillary channels. When the expansion angle of the stop valve is 170°, and the concentration of PEO is 0.2% or 0.4%, the stationary time in this experiment can be greater than 30 minutes until the DI water dries completely. However, the stop valve with the 170° expansion angle will not work perfectly when the contact angle of the PEO-PDMS is less than 45°. The fluid meniscus holding time at the opening of the valve is important for one reagent sample mixing with another one. It can provide enough time for the two or more different reagents mixing or reaction in the chamber. Then, the fluid flow resumes advancing in the channel for the next step's motion.

**Table 2.** The fluid stationary time for the stop valves with six different expansion angles and the PEO-PDMS cover in the 0.4% PEO concentration

Capillary stop valve expansion angles (degree)	Stationary time
60	0
90	0
110	2 min
130	4 min
150	15 min
170	More than 40 min

**Table 3.** The fluid stationary time for the stop valves with the same 170° expansion angle and the PEO-PDMS covers in five different PEO concentrations

Concentrations of PEO	Contact angles of PEO-PDMS (degree)	Stationary time
0.2%	80.9	More than 40 min
0.4%	58.5	More than 40 min
0.6%	50.3	15 min
0.8%	43.8	5 min
>1.0%	< 45.3	0

**Table 4.** The fluid stationary time is for the stop valves with the same 170° expansion angle and the same depth of 100 μm but the valve having three different aspect ratios of the patterns. The PEO-PDMS cover is in the 0.4% PEO concentration.

Widths of the capillary channels (μm)	Velocity(μm/s)	Stationary time
50	79.7	32 min
100	120.4	28 min
150	435.8	15 min

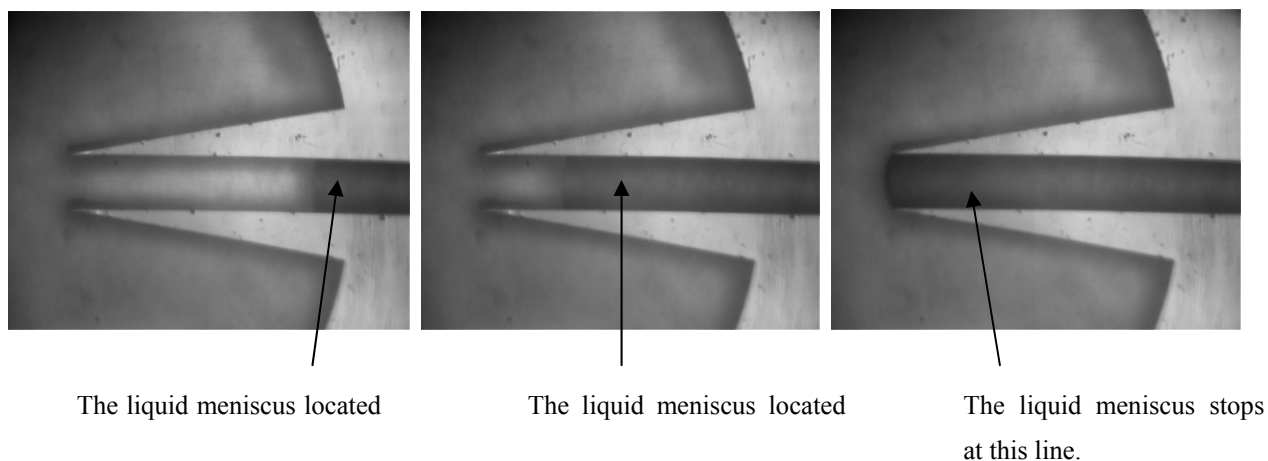
**Table 5.** The fluid stationary time is for the stop valves with the same 170° expansion angle and the same width of 100 μm but the valve having three different aspect ratios of the patterns. The PEO-PDMS cover is in the 0.4% PEO concentration.

Depths of the capillary channels (μm)	Velocity (μm/s)	Stationary time
50	329.6	8 s
100	120.4	28 min
150	19.5	35 min

We also found if the PEO concentrations are 1.0%–1.9%, the capillary action works well, but the microvalve does not work. However, if the PEO concentrations are 0.2%–0.8%, the fluid can still flow smoothly in the microchannel with the capillary action and the microvalve functions well. Finally, the fluid successfully stops at the opening of the valve, but the flow rate may be slower than the higher concentrations of PEO. These results indicate that the surface tension at the stop valve must achieve balance in order to make the capillary action work and the stop valve work as well. The adjustable surface tension of PEO-PDMS and the aspect ratio of the microchannel provide an effective method to control this balance for different applications. Currently, there are many other studies for the fluid flow. These studies describe the phenomenon of the fluid flow in the capillary channel and stop valve

considered in this work. Our proposed methods are easily fabricated and sealed, as well as beneficial to a wide range of biomedical analysis testing systems in related fields.

**Figure 13.** The three images under a microscope show the different positions of the liquid meniscus moving in the capillary channel and finally stop at the opening of the passive valve (colored DI water is the testing sample). These image sequences demonstrate the fluid flowing in the microchannel. The capillary channel (230  $\mu\text{m}$  deep, 20  $\mu\text{m}$  wide) is connected to a stop valve of an expanding angle 170°.



#### 4. Conclusions

A high sensitivity, low cost and miniaturized optical system with an autonomous fluid manipulation chip was successfully developed and tested. To insure the high sensitivity, superbright LED and highly sensitive photodiode with integrated preamplifier are accepted as the light source and detection sensor. Meanwhile, these two parts and all necessary optical elements are integrated into one small package about 2 cm  $\times$  2 cm  $\times$  2 cm. As we know, this system has the highest sensitivity in the smallest package, which has not been published until now. This prototype was tested using fluoresce dye 5-Carboxyfluorescein (5-FAM) dissolved in solvent DMSO (Dimethyl Sulfoxide) and then diluted with DI water in various ratios as the testing solution samples. The testing results prove a remarkable sensitivity at the pico-scale molar around 1.08 pM. This sensitivity range should meet most of the bio-detection requirements. The cost-effective fluorescence detection system, described in this paper, can be easily integrated with the microchip, lab-on-a-chip, portable fluorescent detection device and systems for biological, chemical, medical and point-of-care applications.

The autonomous fluid manipulation chip includes a capillary stop valve with an adjustable surface tension PEO-PDMS which has been successfully fabricated and tested. The design of the stop valve can be manipulated to control the fluid meniscus stationary time from two minutes to more than half an hour by changing the aspect ratio of the microchannel, the expansion angle of the channel cross-section at the end of the capillary channel, and the contact angle of the PEO-PDMS. The testing results are also presented in detail under different designs: the aspect ratio from 2 to 0.67, the valve expanding angle from 60° to 170°, and the contact angle of PEO-PDMS from 21.5° to 80.9°. In these experiments, the capillary stop valves are fabricated by photolithography, ICP dry etching, and sealed with the PEO-PDMS as a cover. Then, they are tested for passing/stopping liquid samples based on

their wettability. If the contact angle of the PEO-PDMS is about  $80.9^\circ$  or  $58.5^\circ$  (0.2% or 0.4% PEO concentration) and the expanding angle is  $170^\circ$ , the fluid can flow smoothly only under the capillary action in the microchannels, and then the meniscus stops at the edge of the microvalve for more than 30 min until the DI water dries completely. This phenomenon can be used for some biochemical applications such as complete mixing and reaction, *etc.* As far as we know, this designed microvalve sealed with the modified PDMS cover has not been previously published. All the experimental data could be used as good references for designers. The testing results indicate the liquid meniscus can stop at the valve opening with differently designed pattern sizes and the PEO-PDMS with different contact angles. This simple and cost-effective capillary stop valve should be an applicable flow control method in microfluidic systems, such as micro assay or lab-on-a-chip systems, which require enough reaction time or incubation time.

## References

1. Srinivasan, V.; Pamula, V.K.; Fair, R.B. An integrated digital microfluidic lab-on-chip for clinical diagnostics on human physiological fluids. *Lab Chip* **2004**, *4*, 310–315.
2. Kostner, S.; Vellekoop, M.J. Detection of single biological cells using a DVD pickup head. In *Proceedings of the IEEE International Solid-State Sensors, Actuators and Microsystems Conference*, Lyon, France, 10–14 June 2007; pp. 2123–2126.
3. Chediak, J.A.; Luoa, Z.; Seo, J.; Cheung, N.; Lee, L.P.; Sandse, T.D. Heterogeneous integration of Cds filters with GaN LEDs for fluorescence detection Microsystems. *Sens. Actuat. A* **2004**, *111*, 1–7.
4. Seo, J.; Lee, L.P. Disposable integrated microfluidics with self-aligned planar microlenses. *Sens. Actuat. B* **2004**, *99*, 615–622.
5. Yang, H.; Lee, C.T. Miniaturized fluorescence excitation platform with optical fiber for bio-detection chips. In *Proceedings of the Microsystem Technologies—Symposium on Design, Test, Integration and Packaging of MEMS/MOEMS*, Stresa, Italy, 26–28 April 2006; pp. 1–5.
6. Kostal, V.; Zeisbergerova, M.; Slais, K.; Kahle, V. Fluorescence detection system for capillary separations utilizing a liquid core waveguide with an optical fibre-coupled compact spectrometer. *Chromatogr. A* **2005**, *1081*, 36–41.
7. Optical Detection Microscopy. Available online: <http://en.wikipedia.org/wiki/Microscopy> (accessed on 10 April 2012).
8. Klotzkin, D.; Papautsky, I. High-sensitivity integrated fluorescence analysis for microfluidic lab-on-a-chip. *SPIE Newsroom* **2007**, doi: 10.1117/2.1200705.0748.
9. Hung, K.Y.; Tseng, F.G.; Khoo, H.S. Integrated three-dimensional optical MEMS for chip-based fluorescence detection. *J. Micromech. Microeng.* **2008**, doi: 10.1088/0960-1317/19/4/045014.
10. Novak, L.; Neuzil, P.; Pipper, J.; Zhang, Y.; Lee, S. An integrated fluorescence detection system for lab-on-a-chip applications. *Lab Chip* **2007**, *7*, 27–29.
11. Shen, B.; Xie, Y.; Irawan, R. A novel portable fluorescence detection system for microfluidic card. *J. Instrument.* **2008**, *3*, 1–11.
12. Chin, C.D.; Linder, V.; Sia, S.K. Lab-on-a-chip devices for global health: Past studies and future opportunities. *Lab Chip* **2007**, *7*, 41–57.

13. Mitchell, P. Microfluidics-downsizing large-scale biology. *Nat. Biotechnol.* **2001**, *19*, 717–721.
14. Kopp, M.U.; Crabtree, H.J.; Manz, A. Developments in technology and applications of Microsystems. *Chem. Biol.* **1997**, *1*, 410–419.
15. Colyer, C.L.; Tang, T.; Chiem, N.; Harrison, D.J. Clinical potential of microchip capillary electrophoresis systems. *Electrophoresis* **1997**, *18*, 1733–1741.
16. Wang, J.; Rivas, G.; Cai, X.; Palecek, E.; Nielsen, P.; Shiraishi, H.; Dontha, N.; Luo, D.; Parrado, C.; Chicharro, M.; Farias, P.; Valera, F.S.; Grant, D.H.; Ozsoz, M.; Flair, M.N. DNA electrochemical biosensors for environmental monitoring—A review. *Anal. Chim. Acta* **1997**, *347*, 1–8.
17. Schult, K.; Katerkamp, A.; Trau, D.; Grawe, F.; Camman, K.; Meusel, M. Disposable optical Sensor chip for medical diagnostics: New ways in bioanalysis. *Anal. Chem.* **1999**, *71*, 5430–5435.
18. Reyes, D.R.; Iossifidis, D.; Auroux, P.A.; Manz, A. Micro total analysis systems: Introduction, theory and technology. *Anal. Chem.* **2002**, *74*, 2623–2636.
19. van de Schoot, B.H.; Verpoorte, E.M.J.; Jeanneret, S.; Manz, A.; Rooij, N.R. Microsystems for analysis in flowing solutions. In *Proceedings of the Micro Total Analysis Systems ( $\mu$ TAS94)*, Twente, The Netherlands, 21–22 November 1994; pp. 181–190.
20. Ramsey, J.M.; Widmer, E.; Verpoorte, E. Miniature chemical measurement systems. In *Proceedings of the 2nd International Symposium on Miniaturized Total Analysis Systems, ( $\mu$ TAS96)*, Basel, Switzerland, 19–22 November 1996; pp. 24–29.
21. Northrup, M.A.; Benett, B.; Hadley, D.; Stratton, P.; Landre, P. Advantages afforded by miniaturization and integration of DNA analysis instrumentation. In *Proceedings of the 1st International Conference on Microreaction Technology*, Frankfurt, Germany, 23–24 February 1997; pp. 278–288.
22. Blankenstein, G.; Larsen, U.D. Modular concept of a laboratory on a chip for chemical and biochemical analysis. *Biosens. Bioelectron.* **1998**, *13*, 427–438.
23. Nilsson, S.; Laurell, T. Miniaturization in analytical and bioanalytical chemistry. *Anal. Bioanal. Chem.* **2004**, *378*, 1676–1677.
24. Nguyen, N.T.; Wereley, S.T. *Fundamentals and Applications of Microfluidics*; Artech House: Boston, MA, USA, 2002.
25. Selvaganathy, P.; Carlen, E.T.; Mastrangelo, C.H. Electrothermally actuated inline microfluidic valve. *Sens. Actuat. A* **2003**, *114*, 275–282.
26. Esashi, M.; Shoji, S.; Nakano, A. Normally closed microvalve and micropump fabricated on a silicon wafer. *Sens. Actuat.* **1989**, *20*, 163–169.
27. Andersson, H.; Wijngaart, W.; Griss, P.; Niklaus, F.; Stemme, G. Hydrophobic valves of plasma deposited octafluorocyclobutane in drier channels. *Sens. Actuat. B* **2001**, *75*, 136–141.
28. Man, P.F.; Mastrangelo, C.H.; Burns, M.A.; Burke, D.T. Microfabricated capillary driven stop valves and sample injector. In *Proceedings of the 11th Annual International Workshop on Micro Electro Mechanical Systems, MEMS Conference*, Heidelberg, Germany, 25–29 January 1998; pp. 25–29.
29. Zoval, J.V.; Madou, M.J. Centrifuge based fluidic platforms. *Proc. IEEE* **2004**, *921*, 140–153.
30. Lauks, I.R.; Wieck, H.J.; Zelin, M.P.; Blyskal, P. Disposable Sensing Device for Real Time Fluid Analysis. U.S. Patent 5,096,669, 17 March 1992.

31. Kugelmass, S.M.; Lin, C.; DeWitt, S.H. Fabrication and characterization of three-dimensional microfluidic arrays. In *Proceedings of the SPIE 3877 on Microfluidics Devices and Systems II*, Santa Clara, CA, USA, 20–21 September 1999; p. 88.
32. McNeely, M.R.; Spute, M.K.; Tusneem, N.A.; Oliphant, A.R. Hydrophobic microfluidics. In *Proceedings of SPIE 3877 on Microfluidic Devices and Systems II*, Santa Clara, CA, USA, 20–21 September 1999; p. 210.
33. Handique, K.; Burke, D.T.; Mastrangelo, C.H.; Burns, M.A. Nanoliter liquid metering in microchannels using hydrophobic patterns. *Anal. Chem.* **2000**, *72*, 4100–4109.
34. Melin, J.; Roxhed, N.; Gimenez, G.; Griss, P.; van der Wijngaart, W.; Stemme, G. A liquid-triggered liquid microvalve for on-chip flow control. *Sens. Actuat. B* **2004**, *100*, 463–468.
35. Dasgupta, P.K.; Eom, I.Y.; Morris, K.J.; Li, J.Z. Light emitting diode-based detectors-absorbance, fluorescence and spectroelectrochemical measurement in a planar flow-through cell. *Anal. Chim. Acta* **2003**, *500*, 337–364.
36. Braunstein, R. Radiative transitions in semiconductors. *Phys. Rev.* **1955**, *99*, 1892–1893.
37. Dereniak, E.L.; Crowe, D.G. *Optical Radiation Detectors*; Wiley: New York, NY, USA, 1984; pp. 57–68.
38. Webb, P.P.; McIntyre, R.J.; Conradi, J. Properties of avalanche photodiodes. *RCA Rev.* **1975**, *35*, 234–278.
39. Laermer, F.; Schilp, A. Method of Anisotropically Etching Silicon. U.S. Patent 5,501,893, 26 March 1996.
40. Laermer, F.; Schilp, A.; Funk, K.; Offenber, M. Bosch deep silicon etching: Improving uniformity and etch rate for advanced mems applications. In *Proceeding of the Technical Digest IEEE International Conference on MEMS '99*, Orlando, FL, USA, 17–21 January 1999; pp. 211–216.
41. Quevy, E.; Parvais, B.; Raskin, J.P.; Buchaillet, L.; Flander, D.; Collard, D. A modified Bosch-type process for precise surface micromachining polysilicon. *J. Micromech. Microeng.* **2002**, *12*, 328–333.
42. Cha, J.H.; Kim, J.; Ryu, S.K.; Park, J.Y.; Jeong, Y.; Park, S.; Park, S.H.; Kim, S.C.; Chun, K.J. A highly efficient 3D micromixer using soft PDMS bonding *J. Micromech. Microeng.* **2006**, *15*, 1778–1782.
43. Egidi, G.; Herrera, F.; Moreno-Bondi, M.C.; Kempe, M.; van Rhijn, J.A.; Fiaccabrino, G.C.; de Rooij, N.F. Fabrication and characterization of stop flow valves for fluid handling. In *Proceedings of the 12th International Conference on Solid-State Sensors, Actuators and Microsystems*, Boston, MA, USA, 8–12 June 2003; pp. 147–150.
44. Dhruv, H.D. Controlling Nonspecific Adsorption of Proteins at Bio-Interfaces for Biosensor and Biomedical Applications. Ph.D. Dissertation, Utah State University, Logan, UT, USA, 2009.
45. Gliere, A.; Delattre, C. Modeling and fabrication of capillary stop valves for planar microfluidic systems. *Sens. Actuat. A* **2006**, *130–131*, 601–608.